Nigerian Journal of Technology (NIJOTECH)
Vol. 44, No. 2, June, 2025, pp.293 - 301
www.nijotech.com

Print ISSN: 0331-8443
Electronic ISSN: 2467-8821
https://doi.org/10.4314/njt.v44i2.13

MODELING AND PERFORMANCE ANALYSIS OF OUTPUT ENHANCED TRANSFER FIELD (TF) MACHINE

AUTHORS:
A. R. Salihu[1,*], and L. U. Anih[2]

AFFILIATIONS:
[1,2]Department of Electrical Engineering, University of Nigeria, Nsukka, 410001 Nsukka, Enugu, Nigeria.

***CORRESPONDING AUTHOR:**
Email: rufai.salihu@unn.edu.ng

ARTICLE HISTORY:
Received: 04 April, 2025.
Revised: 10 June, 2025.
Accepted: 17 June, 2025.
Published: 07 July, 2025.

KEYWORDS:
Transfer field, Rotor induced currents, Capacitance injection, Coupled machine, Swapped windings, Improved outputs.

ARTICLE INCLUDES:
Peer review

DATA AVAILABILITY:
On request from author(s)

EDITORS:
Ozoemena Anthony Ani

FUNDING:
None

Abstract

The output performance of a conventional transfer field (TF) machine is low in comparison with those of other asynchronous machines. In this study, a reconfigured transfer field machine with simultaneous rotor induced currents and capacitance injection for enhancement is presented. The machine comprises two identical salient-pole machine elements that are coupled mechanically and wound integrally for the same pole number. The salient-pole half axes are displaced in space quadrature in the machine elements comprising the machine. Each stator has dual sets of identical poly-phase windings regarded as primary and secondary that are sinusoidally distributed in the stator slots. Primary windings are interconnected in series between the machine elements and the terminals connected to public utility source while the secondary windings are swapped betwixt the machine elements and then terminated on a balanced variable capacitor bank. Windings are also placed on the rotors. The mathematical model of the machine is derived, the resulting equations therefrom are simulated in MATLAB/Simulink environment. It is shown that with an optimized value of $8{,}300\mu F$ *tuned capacitor, a remarkable improvement in the performance characteristics of the machine over the traditional TF machine is obtained when compared. The starting torque, power factor and maximum torque increased by 384.2% (1.9N-m to 9.2N-m), 87.5% (0.32 to 0.6) and 374.1% (6N-m to 28.45N-m) respectively, which confirm superior performance characteristics.*

1.0 INTRODUCTION

Induction motors are more widely used in industries for electro-mechanical energy conversion than any other energy conversion device. Its relative cheapness, ruggedness, easy maintainability and self-starting features are the characteristic attributes which have endeared the machines to the industries. Another energy conversion device type in similitude to the induction motor is the transfer–field (TF) machine. Both are asynchronous, self-starting and have similar torque-speed characteristics, although the synchronous speed of the TF machine is half $(\omega_o/2)$ that of a typical induction motor. These inherent characteristic features endear the TF machine to low speed applications much needed in home appliances and other areas where low speed machine is desired [1, 2]. The machine has low output torque on account of its inherent high leakage reactance [3]. The output power of a normal transfer – field machine is much less than that of an induction motor of the same

HOW TO CITE:
Salihu, A. R., and Anih, L. U. "Modeling and Performance Analysis of Output Enhanced Transfer Field (TF) Machine", *Nigerian Journal of Technology*, 2025; 44(2), pp. 293 – 301; https://doi.org/10.4314/njt.v44i2.13

dimension, being about one–third [4]. The high leakage reactance is on the following accounts:

(a) the intersegment conductors between the two machine elements comprising the machine, which are not required in energy transformation,
(b) the two machine elements connected in cascade lead to double end winding leakage flux and the associated reactance,
(c) the two windings occupying same slots imply deeper slots and the attendant higher leakage reactance.

The analyses of the machine as presented in [5, 6] show that the q-axis reactance adds up to the normal leakage reactance of the machine. The overall effects of the high leakage reactance are low output power and efficiency. Furthermore, TF machine draws higher magnetizing current than induction motor from the utility supply in order to operate and consequently, operates at a very low power factor especially at starting and under light load condition [7]. At starting, the power factor is about 0.2 and increases to 0.32 at rated speed if the motor is properly loaded. For these flaws, the machine has been confined to laboratories and research focus on it is scant.

There have been attempts to boost the characteristics of the transfer field (TF) machine in various ways. Researcher [8] tried to improve the output power of the machine by introducing slip frequency voltage of $(2s-1)\omega_o$ into the secondary winding of the machine utilizing solid-state elements. The introduced voltage into the secondary winding was required to supplement the induced voltage into the secondary winding from the primary winding of the TF machine. Thus, the secondary winding current is raised, and by transformer action, a comparable current is taken by the primary winding which is connected to the public utility source for mmf balance; thereby boosting the output power of the machine. The technique nonetheless, never enhanced the torque at starting of the machine. There have also been efforts to inject capacitance directly into the secondary winding, which is electrically detached from the primary winding of the TF machine but magnetically coupled to it [9]. By varying the capacitance of the introduced capacitor, the high leakage reactance of the machine is highly attenuated, depending on the value of the capacitor chosen. The concomitant effect of the reduced reactance of the machine is the resultant increment in power output of the machine. However, the torque at starting did not show any significant increment. Attempt was as well made to introduce induced rotor currents by means of placing winding on the rotor of the TF machine [10 – 12]. The scheme did not indicate appreciable increase in the starting torque as well.

In the present study, rotor induced currents and capacitance injection are simultaneously applied to the machine for reactive power compensation, with a view to improving the power factor, starting torque and for overall improved performance. The performance characteristics of the proposed machine will be compared with those of the primitive TF machine to highlight the superior output performance characteristics over the primitive machine.

2.0 PHYSICAL CONFIGURATION OF THE TF MACHINE

The machine is composed of two similar salient-pole machine elements whose shafts are coupled together mechanically but their pole axes are in space quadrature. Each component machine constituting the TF machine has dual sets of three-phase windings regarded as primary and secondary windings. The two winding sets are magnetically coupled but detached electrically. The axes of primary windings are aligned in series and connected to the public utility source while the secondary windings are swapped betwixt the component machines and then short-circuited. Unlike the conventional TF machine, windings are introduced in the rotor that span both sections of the machine elements. Furthermore, balanced capacitors are introduced in the secondary windings. The primary and secondary windings are all allocated in the stator slots only such that corresponding phases take up selfsame slot positions for utmost coupling. The connection plan of the machine now is presented in Figure 1.

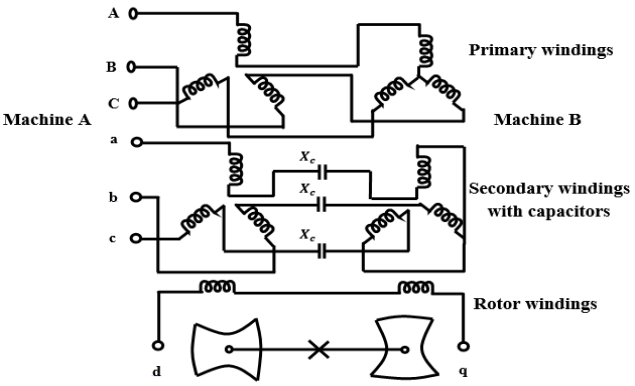

Figure 1: Connection plan of the new TF machine.

3.0 METHODOLOGY

3.1 Model of the TF Machine

The windings are sinusoidally distributed on the stator and rotor slots of the machine. The voltage equations of the machine are stated as:

$$V_{ABC} = R_{ABC} i_{ABC} + p\lambda_{ABC} \quad (1)$$

$$V_{abc} = r_{abc}i_{abc} + p\lambda_{abc} + V_c^{abc} \quad (2)$$
$$V_{qdr} = r_{qdr}i_{qdr} + p\lambda_{qdr} \quad (3)$$

Equations (1) – (2) are for primary and secondary winding voltages while equation (3) is for rotor winding voltage, where

$$\begin{cases} V_{ABC}^T = [V_A \quad V_B \quad V_C] \\ V_{abc}^T = [V_a \quad V_b \quad V_c] \\ V_{qdr}^T = [V_{qr} \quad V_{dr}] \end{cases} \quad (4)$$

$$\begin{cases} R_{ABC} = diag[R_A \quad R_B \quad R_C] \\ r_{abc} = diag[r_a \quad r_b \quad r_c] \\ r_{qdr} = diag[r_{qr} \quad r_{dr}] \end{cases} \quad (5)$$

$$\begin{cases} i_{ABC}^T = [i_A \quad i_B \quad i_C] \\ i_{abc}^T = [i_a \quad i_b \quad i_c] \\ i_{qdr}^T = [i_{qr} \quad i_{dr}] \end{cases} \quad (6)$$

$$\begin{cases} \lambda_{ABC}^T = [\lambda_A \quad \lambda_B \quad \lambda_C] \\ \lambda_{abc}^T = [\lambda_a \quad \lambda_b \quad \lambda_c] \\ \lambda_{qdr}^T = [\lambda_{qr} \quad \lambda_{dr}] \end{cases} \quad (7)$$

$$p = \frac{d}{dt} \text{ and } V_c^{abc} = [V_{c_a} \quad V_{c_b} \quad V_{c_c}]^T \quad (8)$$

The equations of flux linkages in the primary, secondary and rotor windings are written as:

$$\lambda_{ABC} = L_{ABC}i_{ABC} + L_{ABCabc}i_{abc} + L_{ABCqdr}i_{qdr} \quad (9)$$
$$\lambda_{abc} = L_{ABCabc}^T i_{ABC} + L_{abc}i_{abc} + L_{abcqdr}i_{qdr} \quad (10)$$
$$\lambda_{qdr} = L_{ABCqdr}^T i_{ABC} + L_{abcqdr}^T i_{abc} + L_{qdr}i_{qdr} \quad (11)$$

The current, i_{abc} in the secondary windings may be related in terms of capacitor voltage and capacitance, C as:

$$i_{abc} = CpV_c^{abc} \quad (12)$$

The self and mutual inductances of primary, secondary and rotor windings are L_{ABC}, L_{abc} and L_{qdr} respectively, while L_{ABCabc} and L_{ABCabc}^T are coupling inductances between the stator windings. The mutual inductances betwixt the rotor and stator windings are L_{ABCqdr}^T and L_{abcqdr}^T.

Note that variables related to primary, secondary and rotor windings are illustrated by scripts ABC, abc and qdr respectively.

These flux linkage equations (9), (10) and (11) can be rewritten as:

$$\begin{bmatrix} \lambda_{ABC} \\ \lambda_{abc} \\ \lambda_{qdr} \end{bmatrix} = \begin{bmatrix} L_{11} & L_{12} & L_{13} \\ L_{21} & L_{22} & L_{23} \\ L_{31} & L_{32} & L_{33} \end{bmatrix} \begin{bmatrix} i_{ABC} \\ i_{abc} \\ i_{qdr} \end{bmatrix} \quad (13)$$

$$L_{11} = \begin{bmatrix} L_{AA} & L_{AB} & L_{AC} \\ L_{BA} & L_{BB} & L_{BC} \\ L_{CA} & L_{CB} & L_{CC} \end{bmatrix}, L_{22} = \begin{bmatrix} L_{aa} & L_{ab} & L_{ac} \\ L_{ba} & L_{bb} & L_{bc} \\ L_{ca} & L_{cb} & L_{cc} \end{bmatrix},$$
$$\text{and } L_{33} = \begin{bmatrix} L_{qr} & L_{qdr} \\ L_{dqr} & L_{dr} \end{bmatrix} \quad (14)$$

$$L_{12} = \pm \begin{bmatrix} L_{Aa} & L_{Ab} & L_{Ac} \\ L_{Ba} & L_{Bb} & L_{Bc} \\ L_{Ca} & L_{Cb} & L_{Cc} \end{bmatrix}, L_{23} = \pm \begin{bmatrix} L_{aqr} & L_{adr} \\ L_{bqr} & L_{bdr} \\ L_{cqr} & L_{cdr} \end{bmatrix}$$
$$\text{and} L_{31} = \begin{bmatrix} L_{qrA} & L_{drA} \\ L_{qrB} & L_{drB} \\ L_{qrC} & L_{drC} \end{bmatrix} \quad (15)$$

The sign $\pm$ in the coupling inductance terms L_{12} and L_{23} are due to the swapping of the secondary windings and as a result, if the mutual coupling inductance is negative in one half of the machine, it is positive in the other and conversely [13 – 15].

The inductance matrix of the primary windings of the TF machine:

$$L_{11}^{Machine\ A} = \begin{bmatrix} L_l + L_o - L_{ms}\cos 2\theta_r & -\frac{1}{2}L_o - L_{ms}\cos(2\theta_r - 2\pi/3) & -\frac{1}{2}L_o - L_{ms}\cos(2\theta_r + 2\pi/3) \\ -\frac{1}{2}L_o - L_{ms}\cos(2\theta_r - 2\pi/3) & L_l + L_o - L_{ms}\cos 2(\theta_r - 2\pi/3) & -\frac{1}{2}L_o - L_{ms}\cos(2\theta_r + 2\pi) \\ -\frac{1}{2}L_o - L_{ms}\cos(2\theta_r + 2\pi/3) & -\frac{1}{2}L_o - L_{ms}\cos(2\theta_r + 2\pi) & L_l + L_o - L_{ms}\cos 2(\theta_r + 2\pi/3) \end{bmatrix} \quad (16)$$

$$L_{11}^{Machine\ B} = \begin{bmatrix} L_l + L_o + L_{ms}\cos 2\theta_r & -\frac{1}{2}L_o + L_{ms}\cos(2\theta_r - 2\pi/3) & -\frac{1}{2}L_o + L_{ms}\cos(2\theta_r + 2\pi/3) \\ -\frac{1}{2}L_o + L_{ms}\cos(2\theta_r - 2\pi/3) & L_l + L_o + L_{ms}\cos 2(\theta_r - 2\pi/3) & -\frac{1}{2}L_o + L_{ms}\cos(2\theta_r + 2\pi) \\ -\frac{1}{2}L_o + L_{ms}\cos(2\theta_r + 2\pi/3) & -\frac{1}{2}L_o + L_{ms}\cos(2\theta_r + 2\pi) & L_l + L_o + L_{ms}\cos 2(\theta_r + 2\pi/3) \end{bmatrix} \quad (17)$$

The L_l in the diagonal elements of the matrices explains the leakage inductance of the winding and considered to be equal for the winding phases. The inductance matrix, L_{11} of the primary winding is the totality of such inductances of machine A and machine B comprising the TF.

$$L_{11} = L_{11}^{Machine\ A} + L_{11}^{Machine\ B} =$$
$$\begin{bmatrix} 2L_l + L_{md} + L_{mq} & -\frac{1}{2}(L_{md} + L_{mq}) & -\frac{1}{2}(L_{md} + L_{mq}) \\ -\frac{1}{2}(L_{md} + L_{mq}) & 2L_l + L_{md} + L_{mq} & -\frac{1}{2}(L_{md} + L_{mq}) \\ -\frac{1}{2}(L_{md} + L_{mq}) & -\frac{1}{2}(L_{md} + L_{mq}) & 2L_l + L_{md} + L_{mq} \end{bmatrix} \quad (18)$$

where, $L_o = \frac{L_{md} + L_{mq}}{2}$ (19)

For the mutual inductance matrix betwixt the primary and secondary windings,

$$L_{12}^{Machine\ A} = \begin{bmatrix} L_l + L_o - L_{ms}\cos 2\theta_r & L_o\cos\alpha - L_{ms}\cos(2\theta_r - \alpha) & L_o\cos\alpha - L_{ms}\cos(2\theta_r + \alpha) \\ L_o\cos\alpha - L_{ms}\cos(\theta_r - \alpha) & L_l + L_o - L_{ms}\cos(2\theta_r + \alpha) & L_o\cos\alpha - L_{ms}\cos 2\theta_r \\ L_o\cos\alpha - L_{ms}\cos(2\theta_r + \alpha) & L_o\cos\alpha - L_{ms}\cos 2\theta_r & L_l + L_o - L_{ms}\cos(2\theta_r - \alpha) \end{bmatrix} \quad (20)$$

$$L_{12}^{Machine\ B} = -\begin{bmatrix} L_l + L_o + L_{ms}\cos 2\theta_r & L_o\cos\alpha + L_{ms}\cos(2\theta_r - \alpha) & L_o\cos\alpha + L_{ms}\cos(2\theta_r + \alpha) \\ L_o\cos\alpha + L_{ms}\cos(\theta_r - \alpha) & L_l + L_o + L_{ms}\cos(2\theta_r + \alpha) & L_o\cos\alpha + L_{ms}\cos 2\theta_r \\ L_o\cos\alpha + L_{ms}\cos(2\theta_r + \alpha) & L_o\cos\alpha + L_{ms}\cos 2\theta_r & L_l + L_o + L_{ms}\cos(2\theta_r - \alpha) \end{bmatrix} \quad (21)$$

$$L_{12} = L_{12}^{Machine\ A} + L_{12}^{Machine\ B} = (L_{mq} - L_{md})\begin{bmatrix} \cos 2\theta_r & \cos(2\theta_r - \alpha) & \cos(2\theta_r + \alpha) \\ \cos(\theta_r - \alpha) & \cos(2\theta_r + \alpha) & \cos 2\theta_r \\ \cos(2\theta_r + \alpha) & \cos 2\theta_r & \cos(2\theta_r - \alpha) \end{bmatrix} \quad (22)$$

where, $L_{ms} = \frac{L_{md} - L_{mq}}{2}$ and $\alpha = 2\pi/3$. (23)

The similarity between the inductance matrices of this machine and those of the normal induction motor elicits some comments. It is noticed from equation (18) that the sum of the primary winding self-inductance matrices of the component machine stacks which constitute the composite machine is independent of rotor position as reported in [16 – 17]. However, (22) which is the mutual inductance matrix of the primary and secondary windings of the TF machine can be seen to be dependent on the rotor angular position. These observations are some of the features the machine has in common with induction motor.

For primary and secondary windings being identical and identical phases occupying selfsame slot positions on the stator, stator-rotor winding mutual inductances are expressed as:

$$L_{13} = L_{23} = \begin{bmatrix} L_{mq}\cos\theta_r & L_{md}\sin\theta_r \\ L_{mq}\cos(\theta_r - \alpha) & L_{md}\sin(\theta_r - \alpha) \\ L_{mq}\cos(\theta_r + \alpha) & L_{md}\sin(\theta_r + \alpha) \end{bmatrix} \quad (24)$$

$$L_{33} = L_{33}^{Machine\ A} + L_{33}^{Machine\ B} = 2\begin{bmatrix} L_{lqr} + L_{qr} & L_{qrdr} \\ L_{drqr} & L_{ldr} + L_{dr} \end{bmatrix} = 2\begin{bmatrix} L_{lqr} + L_{qr} & 0 \\ 0 & L_{ldr} + L_{dr} \end{bmatrix} \quad (25)$$

where, L_{lqr} and L_{ldr} report the leakage inductances of the rotor windings. Coupling inductances, L_{qrdr} and L_{drqr} between the windings of the rotor along d −axis and q −axis are zeros as a result of the 90^0 angular displacement.

Transformation of stator quantities to arbitrary qdo reference frame is given by [18] using transformation matrices:

$$[K_{S(\theta)}] = \frac{2}{3}\begin{bmatrix} \cos\theta & \cos\left(\theta - \frac{2\pi}{3}\right) & \cos\left(\theta + \frac{2\pi}{3}\right) \\ \sin\theta & \sin\left(\theta - \frac{2\pi}{3}\right) & \sin\left(\theta + \frac{2\pi}{3}\right) \\ \frac{1}{2} & \frac{1}{2} & \frac{1}{2} \end{bmatrix} \quad (26)$$

$$[K_{S(\theta)}]^{-1} = \begin{bmatrix} \cos\theta & \sin\theta & 1 \\ \cos\left(\theta - \frac{2\pi}{3}\right) & \sin\left(\theta - \frac{2\pi}{3}\right) & 1 \\ \cos\left(\theta + \frac{2\pi}{3}\right) & \sin\left(\theta + \frac{2\pi}{3}\right) & 1 \end{bmatrix} \quad (27)$$

Employing $K_{S(\theta)}$ to voltage equation (1) of the primary winding gives

$V_{QDO} = [K_S]P[K_S]^{-1}\lambda_{QDO} + [K_S]\mathrm{R}[\mathrm{K_S}]^{-1}i_{QDO}$ (28)

$V_Q = Ri_Q + \omega\lambda_D + p\lambda_Q$ (29)

$V_D = Ri_D - \omega\lambda_Q + p\lambda_D$ (30)

$V_O = Ri_O + p\lambda_O$ (31)

where, R is the entirety of the resistances of the primary windings of both machine elements.

In the same manner, transformation of rotor quantities is stated by [18] using transformation matrices:

$$[K_{R(\beta)}] = \frac{2}{3}\begin{bmatrix} \cos\beta & \cos\left(\beta - \frac{2\pi}{3}\right) & \cos\left(\beta + \frac{2\pi}{3}\right) \\ \sin\beta & \sin\left(\beta - \frac{2\pi}{3}\right) & \sin\left(\beta + \frac{2\pi}{3}\right) \\ \frac{1}{2} & \frac{1}{2} & \frac{1}{2} \end{bmatrix} \quad (32)$$

where, $\beta = 2\theta_r - \theta$ (33)

$$[K_{R(\beta)}]^{-1} = \begin{bmatrix} \cos\beta & \sin\beta & 1 \\ \cos\left(\beta - \frac{2\pi}{3}\right) & \sin\left(\beta - \frac{2\pi}{3}\right) & 1 \\ \cos\left(\beta + \frac{2\pi}{3}\right) & \sin\left(\beta + \frac{2\pi}{3}\right) & 1 \end{bmatrix} \quad (34)$$

Again, employing $K_{R(\beta)}$ to voltage equation (2) of the secondary winding gives

$V_q = ri_q - (\omega - 2\omega_r)\lambda_d + p\lambda_q + V_{cq}$ (35)

$V_d = ri_d + (\omega - 2\omega_r)\lambda_q + p\lambda_d + V_{cd}$ (36)

$V_o = ri_o + p\lambda_o$ (37)

where, r is the entirety of the resistances of the secondary windings of both machine elements, V_{cq} and V_{cd} in equations (35) and (36) are capacitor voltages.

Analogously, the rotor winding voltage can be expressed as:

$V_{qr} = r_r i_{qr} + (\omega - 2\omega_r)\lambda_{dr} + p\lambda_{qr}$ (38)

$$V_{dr} = r_r i_{dr} - (\omega - 2\omega_r)\lambda_{qr} + p\lambda_{dr} \quad (39)$$

where, r_r is also the entirety of the resistances of the rotor windings in both machine elements.

The V_{cq} and V_{cd} in equations (35) and (36) may be expressed as:

$$\begin{cases} pV_{cq} = \frac{i_q}{C} - (\omega - 2\omega_r)V_{cd} \\ pV_{cd} = \frac{i_d}{C} + (\omega - 2\omega_r)V_{cq} \end{cases} \quad (40)$$

Employing $K_{S(\theta)}$ to ABC flux linkage of (9) and (13) of the primary winding gives:

$$\lambda_{QDO} = [K_{S(\theta)}]L_{11}[K_{S(\theta)}]^{-1} i_{QDO} + [K_{S(\theta)}]L_{12}[K_{R(\beta)}]^{-1} i_{qdo} + [K_{S(\theta)}]L_{13} i_{qdr} \quad (41)$$

$$\lambda_Q = 2(L_l + L_{md})i_Q + (L_{mq} - L_{md})(i_Q + i_q + i_{qr}) \quad (42)$$

$$\lambda_D = 2(L_l + L_{mq})i_D + (L_{md} - L_{mq})(i_D + i_d + i_{dr}) \quad (43)$$

$$\lambda_O = 2L_l i_O \quad (44)$$

In a similar fashion, employing $K_{R(\beta)}$ to abc flux linkage of (10) and (13) of the secondary winding gives:

$$\lambda_{qdo} = [K_{R(\beta)}]L_{21}[K_{S(\theta)}]^{-1} i_{QDO} + [K_{R(\beta)}]L_{22}[K_{R(\beta)}]^{-1} i_{qdo} + [K_{R(\beta)}]L_{23} i_{qdr} \quad (45)$$

$$\lambda_q = 2(L_l + L_{md})i_q + (L_{mq} - L_{md})(i_q + i_Q + i_{qr}) \quad (46)$$

$$\lambda_d = 2(L_l + L_{mq})i_d + (L_{md} - L_{mq})(i_d + i_D + i_{dr}) \quad (47)$$

$$\lambda_o = 2L_l i_o \quad (48)$$

In a like manner, the rotor winding qdr flux linkage of (11) and (13) may be expressed as:

$$\lambda_{qdr} = L_{31}[K_{S(\theta)}]^{-1} i_{QDO} + L_{32}[K_{R(\beta)}]^{-1} i_{qdo} + L_{33} i_{qdr} \quad (49)$$

$$\lambda_{qr} = (2L_{lr} + L_m)i_{qr} + (L_{mq} - L_{md})(i_{qr} + i_Q + i_q) \quad (50)$$

$$\lambda_{dr} = (2L_{lr} + L_m)i_{dr} + (L_{md} - L_{mq})(i_{dr} + i_d + i_D) \quad (51)$$

where, $L_m = L_{mq} - L_{md}$ (52)

The electromagnetic torque can be derived considering the energy available in the air gap as:

$$T_e = \frac{n}{2}\left\{\left[(K_{S(\theta)})^{-1} i_{QDO}\right]^T \frac{\partial[L_{12}]}{\partial\theta_r}(K_{R(\beta)})^{-1} i_{qdo} + \left[(K_{S(\theta)})^{-1} i_{QDO}\right]^T \frac{\partial[L_{13}]}{\partial\theta_r} i_{qdr} + \left[(K_{R(\beta)})^{-1} i_{qdo}\right]^T \frac{\partial[L_{23}]}{\partial\theta_r} i_{qdr}\right\} \quad (53)$$

Equation (53) may be stated in terms of inductance and current as:

$$T_e = \frac{3}{2}\left(\frac{n}{2}\right)(L_{md} - L_{mq})[(i_Q i_d + i_q i_D) + (i_Q i_{dr} + i_{qr} i_D) + (i_q i_{dr} + i_{qr} i_d)] \quad (54)$$

where, n is the pole number of the machine.

The torque produced is consequent upon the interactions betwixt and among the primary winding, secondary winding and rotor winding.

3.2 Simulation of the TF Machine

The simulation of the model TF and conventional TF machines was accomplished on MATLAB/Simulink environment. Synchronously rotating reference frame was adopted. This was effected by relating the ω in arbitrary reference frame to ω_s [19], while ω_s is the synchronous speed. The simulation was conducted with simulink model for a computer time of two (2) seconds.

The different starting transients of the two machines were noticed during simulations. The results of the simulation were observed with the use of simulink scopes to be satisfactorily in order. A load torque of 2N-m was introduced at one (1) second when the motors have reached a full speed and transients had eased off. The performance characteristics of the machines were then observed.

The circuit parameters for the proposed TF machine modified from the conventional machine presented by [6] are shown in Table 1. The parameters given in Table 1 are for one machine element.

Table 1: Circuit parameters of the newly modeled TF machine [6]

Parameters	Values
L_{md}	133.3× 10^{-3} (H)
L_{mq}	25.6× 10^{-3} (H)
L_l	6.0× 10^{-3} (H)
$R = r = r_r$	3.0 (Ω)
J	1.98 × 10^{-3} (Kgm^2)
V	220 (V)
n	4

3.3 Steady-State Model of the TF Machine

The equations of the steady state performance of the new TF machine may be drawn by subjecting all time varying components of the voltage equations (29) to (31), (35) to (37) and, (38) and (39) to zero. The d – axis equations reduce to:

$$\begin{cases} V_D = Ri_D - \omega\lambda_Q \\ V_d = ri_d + (\omega - 2\omega_r)\lambda_q + V_{cd} \\ V_{dr} = r_r i_{dr} - (\omega - 2\omega_r)\lambda_{qr} \end{cases} \quad (55)$$

To set the d – axis to be aligned with the a-phase, the ensuing relationships coexist betwixt the q- and d-axes variables;

$$\begin{cases} K_D = jK_Q & \text{(Circuit of primary winding)} \\ K_d = -jK_q & \text{(Circuit of secondary winding)} \\ K_{dr} = jK_{qr} & \text{(Circuit of rotor winding)} \end{cases} \quad (56)$$

where, K may be flux linkage, current or voltage as the case may be.

As d – axis is put in order with phase a, accordingly

$$V_D = V_A,\ i_D = i_A,\ i_d = i_a,\ i_{dr} = i_{ar} \text{ and } \omega = \omega_s \quad (57)$$

Therefore, in the primary winding,

$$V_A = Ri_A + j2(X_q)i_A + j(X_{md} - X_{mq})(i_A + i_a + i_{ar}) \quad (58)$$

where, $j\omega_s L = jX_L$ and $X_q = X_l + X_{mq}$

In like manner, it can be revealed that for secondary winding,

$$\frac{V_a}{(2s-1)} = \frac{ri_a}{(2s-1)} + j2(X_q)i_a + j(X_{md} - X_{mq})(i_a + i_A + i_{ar}) - \frac{jX_C i_a}{(2s-1)^2} \quad (59)$$

where, s is slip and $\frac{1}{j\omega_s C} = -jX_C$.

Analogously, for rotor winding,

$$\frac{V_{ar}}{(2s-1)} = \frac{r_r}{(2s-1)} i_{ar} + j(X_r)i_{ar} + j(X_{md} - X_{mq})(i_{ar} + i_a + i_A) \quad (60)$$

where, $X_r = 2X_{lr} + X_m$

Equations (58), (59) and (60) imply the steady-state equivalent circuit in Figure 2a. Figure 2b is the steady-state corresponding circuit while the secondary and rotor windings are short-circuited.

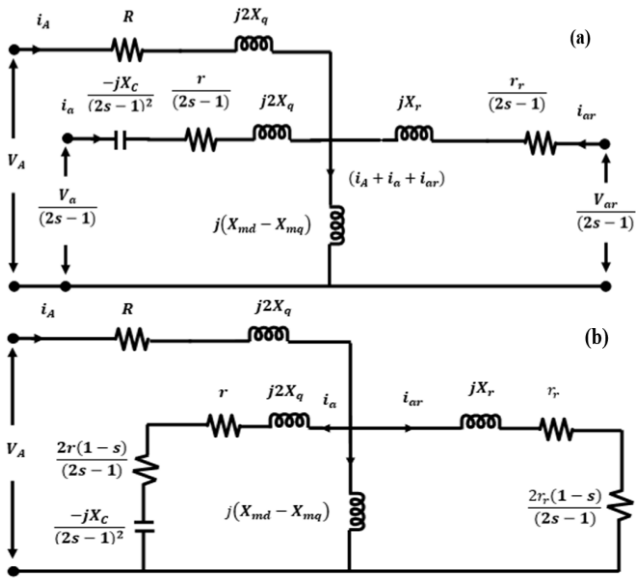

Figure 2: Steady-state equivalent circuit of the new TF machine

The input (equivalent) impedance may be obtained by simple approach of circuit theory and given as:

$$Z = R + j2X_q + (Z_a // Z_1) = R + j2X_q + \frac{Z_a \times Z_1}{Z_a + Z_1} \quad (61)$$

where, $Z_a = j2X_q - \frac{jX_C}{(2s-1)^2} + \frac{r}{(2s-1)}$; $Z_r = \frac{r_r}{(2s-1)} + jX_r$ (62)

$$Z_m = j(X_{md} - X_{mq}); \; Z_1 = \frac{Z_r \times Z_m}{Z_r + Z_m} \quad (63)$$

The steady state torque is the totality of torques developed at both secondary and rotor windings and may be expressed by:

$$T = 6\frac{i_a^2}{\omega_s}\frac{r}{(2s-1)} + 6\frac{i_{ar}^2}{\omega_s}\frac{r_r}{(2s-1)} = 6\frac{r}{\omega_s(2s-1)}[i_a^2 + i_{ar}^2] \quad (64)$$

where, $r = r_r$, i_a and i_{ar} winding resistance, secondary and rotor winding currents respectively.

The power factor of the new machine can easily be obtained from theory of ac circuit as:

$$\text{Power factor, } \cos\varphi = \frac{Real(Z)}{Abs(Z)} = \frac{Real\left[R + j2X_q + \frac{Z_a \times Z_1}{Z_a + Z_1}\right]}{Abs\left[R + j2X_q + \frac{Z_a \times Z_1}{Z_a + Z_1}\right]} \quad (65)$$

4.0 RESULTS AND DISCUSSION

The run-up speed characteristics of the TF machines are shown in Figure 3. The simulation of the machines was carried out to begin on no-load and then accelerated to half of the synchronous speed.

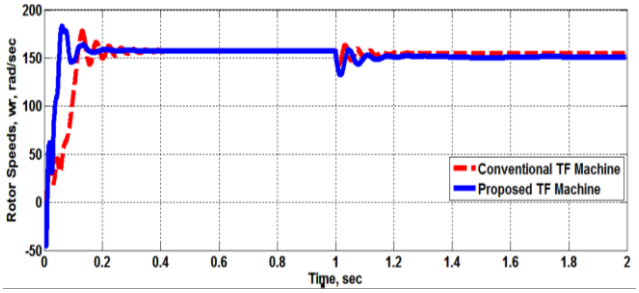

Figure 3: Conventional TF and proposed TF machines' rotor speed characteristics

These speed characteristics of the two machines are similar to each other. However, the new machine has shorter transient period and settled down quickly even after the employment of load. It is noted that the normal TF took about 0.4 second to attain a synchronous speed of 157.08 radians per second after having initial a higher speed transient rises of 176.1 radians per second at start-up. On the other hand, the proposed TF reached a synchronous speed of 157.079 radians per second at an earlier time of 0.3 seconds, after an initial transient speed rise of 180.0 radians per second.

On application of load torque at 1 second, a speed transient rise of 159.2 radians per second was observed for the conventional TF which later settled at a synchronous speed of 149.4 radians per second at 1.25 seconds. Whereas, the proposed TF at the introduction of load had a speed transient rise of 157.18 radians per second and later settled at a synchronous speed of 149.35 radians per second at 1.2 seconds.

Figure 4 presents the characteristics of the primary and secondary winding currents of the conventional TF machine and modeled TF machine with rotor winding and capacitance injection against time for phase A only; (a) is for primary windings, while (b) is for secondary windings of the two TF machines.

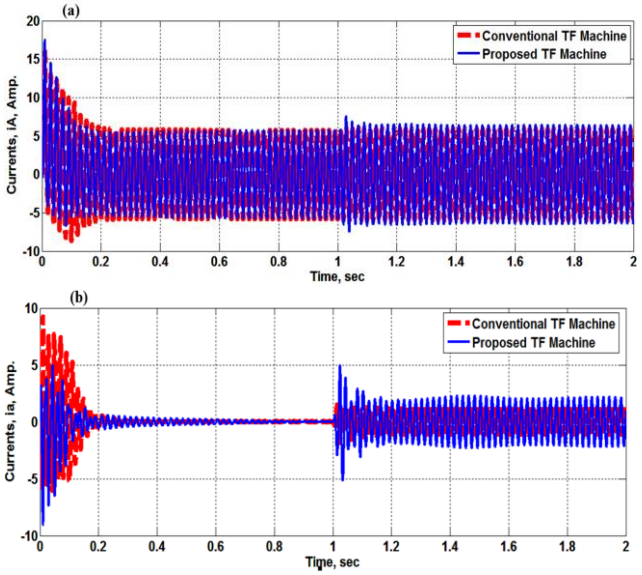

Figure 4: Conventional TF and proposed TF machines' primary and secondary winding currents

In Figure 4, it is visibly clear that for the new TF machine, the currents of the windings have shorter transient time, which suggests that an online starting of the machine can simply be achieved with no serious disturbance to supply. Furthermore, there is a rise in both primary and secondary winding currents of the proposed machine and is clearer during load application, implying greater output power. The rotor currents of the new TF machine model are as well presented in Figure 5. While (a) is for the rotor d – axis current, (b) is for the rotor q – axis current.

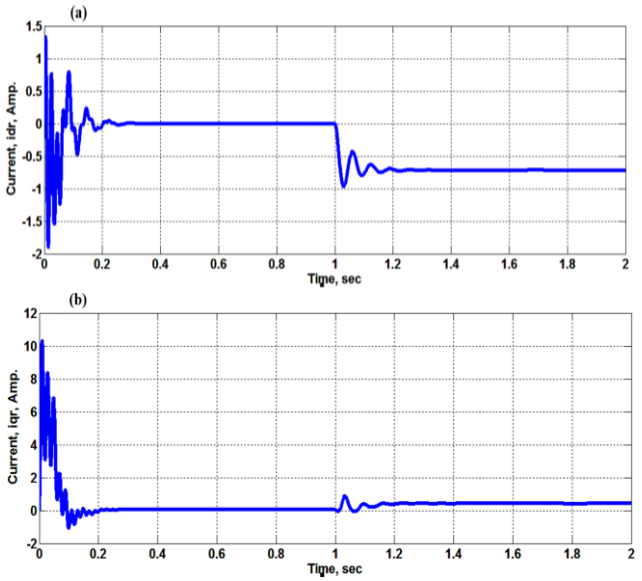

Figure 5: Proposed TF machine rotor d-q currents

Plots of the torque – speed characteristics of the conventional TF and the proposed TF machines are indicated in Figure 6. It is seen that the conventional TF machine has more oscillations before attaining synchronous speed of 157.1 radians per second at zero torque than the proposed TF machine. This shows how the proposed machine is more stable.

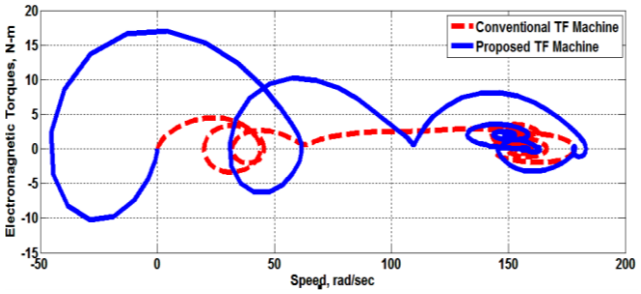

Figure 6: Conventional TF and proposed TF machines' torque – speed characteristics

On employment of load torque, however, the machines swung and settled at speed of 149.3 radians per second while the load torque is 2N-m. The Figure 6 reveals improvement in torque of the new TF machine.

Figure 7 reveals the plots of the steady state torque versus slip of the conventional TF machine and the proposed TF machine. The torque – slip curve of TF machine is analogous to that of an induction motor beside that the synchronous speed of TF is $\omega/2$. This infers that at slip s = 0.5, that is, at speed $\omega_r = \omega/2$, the torque is zero, given that the secondary winding current is zero.

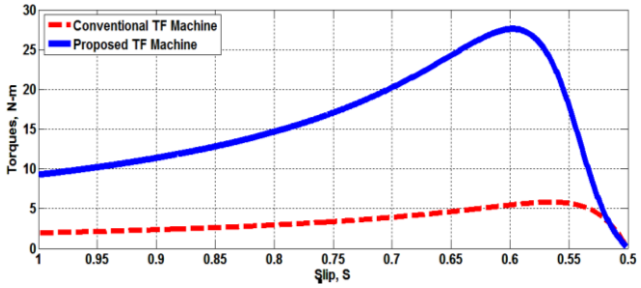

Figure 7: Conventional TF and proposed TF machines' torque – slip curves

It is seen clearly in Figure 7 that the new machine has higher starting and pullout torques.

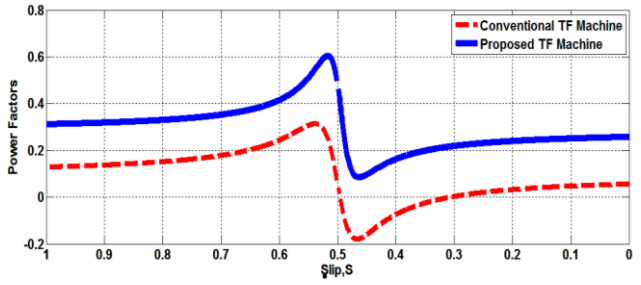

Figure 8: Conventional TF and proposed TF machines' power factor – slip curves

The plots of the power factors of the conventional TF and Proposed TF machines are indicated in Figure 8.

It is noted that the power factor of the new TF machine is superior to that of the conventional counterpart. Both Figures 7 and 8 display the new machine performance conspicuously enhanced.

5.0 CONCLUSION

A new transfer field (TF) machine with enhanced output performance by rotor induced currents and capacitance injection is modeled and the performance analysis has been successfully carried out. The introduced rotor winding current increased the induced electromotive force (EMF) in the machine and lowered the winding impedance. This impedance reduction was accentuated by the negative capacitive reactance of the secondary winding, thus lowering the overall impedance of the machine and resulting in high output performance as indicated in Figures 7 and 8. The juxtaposition of the simulation results of the new TF machine and the conventional counterpart is made. The two machines exhibit performance attributes highly analogous to those of induction motor that is wound for double the pole number. The performance characteristics at start-up and on application of load torque after 1 second reveal the better performance of the new TF machine. Although new machine indicated relative higher transients at start but for a shorter duration. The enhanced performance of the new TF machine is accompanied with increased outputs at improved power factor. With this enhancement, the machine can compete favourably with induction motors of comparable size. One special merit of TF machine is for control purposes. The terminals of the secondary windings can be located outside the machine where the input signal for control studies can be more conveniently applied.

REFERENCES

[1] Obute, K. C., Agu, V. N., Anazia, E. A., Okozi, S. O. and Anih, L. U. "Starting, Steady-State Modelling and Simulation Studies of Single-Phase Transfer-Field Reluctance Motor, Operating in the Asynchronous Mode", *The International Journal of Scientific and Research Publications*, vol. 7, no. 1, pp. 182 – 189, Jan. 2017.

[2] Anih, L. U., and Obute, K. C. "Steady-State Performance Characteristics of Single-Phase Transfer-Field Machine Operating in the Asynchronous Mode", *Nigeria Journal of Technology (NIJOTECH)*, vol. 31, no. 3, pp. 219 – 226, Nov. 2012.

[3] Idoko, H. C., and Anih, L. U. "Modelling and Analysis of a Transfer Field Machine with Displaced Windings", *Institute of Electrical and Electronics Engineers (IEEE) PES/IAS PowerAfrica Conference*, pp. 390 – 395, 2019. DOI: 10.1109/PowerAfrica.2019.8928800

[4] Obute, K. C., Olufolahan, O., Eleanya, M. N., and Anionovo, U. E. "A Novel Three-Phase Transfer Field Reluctance Motor – An Evaluation of Its Performance Characteristics", *Iconic Research and Engineering Journals*, vol. 3, no. 9, pp. 242 – 255, Mar. 2020.

[5] Cathey, J. J., and Nasar, A. A. "Equivalent Circuit of Transfer Field Machine for Asynchronous Mode of Operation", *Electric Machines and Electromechanics*, vol. 6, no. 4, pp. 307 – 321, 1981. https://doi.org/10.1080/03616968108960072

[6] Anih, L. U., and Obe, E. S. "Performance Analysis of a Composite Dual-Winding Reluctance Machine", *Energy Conversion and Management*, vol. 50, no. 12, pp. 3056 – 3062, 2009.https://doi.org/10.1016/j.enconman.2009.08.008

[7] Jimoh, A. A., and Nicolae, D. V. "Controlled Capacitance Injection into a Three-Phase Induction Motor through Single-Phase Auxiliary Stator Winding", *Electric Machines and Drives Conference*, pp. 1183 – 1188, 2007. DOI: 10.1109/IEMDC.2007.383598

[8] Nonaka, S., and Kawaguchi, T. "Variable-Speed Control of Brushless Half-Speed Synchronous Motor by Voltage Source Inverter", *Institute of Electrical and Electronics Engineers (IEEE) Transction on Industry Applications*, vol. 27, no. 3, pp. 545 – 551, May/Jun. 1991. DOI: 10.1109/28.81840

[9] Obe, E. S., and Anih, L. U. "Enhancement of the Performance of a Transfer Field Electric Machine Operating in the Asynchronous Mode", *Nigerian Journal of Technology (NIJOTECH)*, vol. 33, no. 3, pp. 252 – 257, 2014. https://doi.org/10.4314/njt.v33i3.2

[10] Obute, K. C., Olufolahan, O., Nwangugu E. C., and Anionovo, U. E. "Improvement on the Output Characteristics of Conventional Three Phase Transfer Field Machine with Cage (Rotor) Windings", *International Journal of Research in Advent Technology*, vol. 8, no. 4, pp. 4 – 16, 2020. https://doi.org/10.32622/ijrat.82202008

[11] Obute, K. C., Anih, L. U., Ezechukwu, A. O., and Okonkwo, M. C. "A Novel Three Phase Transfer Field Machine with Cage (Rotor) Windings", *The International Journal of*

Engineering and Science (IJES), vol. 9, no. 3, pp. 13 – 31, 2020. DOI: 10.9790/1813-0903011331

[12] Agu, L. A. "Output Enhancement in the Transfer-Field Machine Using Rotor Circuit Induced Currents", *Nigerian Journal of Technology (NIJOTECH)*, vol. 8, no. 1, pp. 7 – 14, Sept. 1984.

[13] Anih, L. U., Obe, E. S., and Abonyi, S. E. "Modelling and Performance of a Hybrid Synchronous Reluctance Machine with Adjustable X_d/X_qratio", *Institute of Engineering and Technolgy (IET) Electric Power Applications*, vol. 9, no. 2, pp. 171 – 182, 2015. DOI: 10.1049/iet-epa.2014.0149

[14] Agbachi, E. O., Anih, L. U., and Obe, E. S., "Steady-State Analysis of Hybrid Synchronous Machine with High Reluctance to Excitation Power Ratio", *Iranian Journal of Electrical and Electronic Engineering*, vol. 18, no. 1, pp. 1 – 12, 2022. https://doi.org/10.22068/IJEEE.18.1.2251

[15] Anih, L. U., Agbachi, E. O., and Obe, E. S., "Dynamic Performance of a Hybrid Synchronous Machine with Ultra – High X_D/X_Q Ratio", *ABUAD Journal of Engineering Research and Development*, vol. 6, no. 1, pp.1–12, 2023.

[16] Anih, L. U., Obe, E. S., and Eleanya, M. N. "Steady – State Performance of Induction and Transfer Field Motors – A Comparison", *Nigerian Journal of Technology (NIJOTECH)*, vol. 34, no. 2, pp. 385 – 391, Apr. 2015. http://dx.doi.org/10.4314/njt.v34i2.24

[17] Anih, L. U., and Agu, L. A. "Mechanism of Torque Production in Coupled Polyphase Reluctance Machine", *Nigerian Journal of Technology*, vol. 27, no. 1, pp. 29 – 39, Mar. 2008.

[18] Krause, P. C., Wasynczuk, O., Sudhoff, S. D. and Pekarek, S. "Analysis of Electric Machinery and Drive Systems", Third Edition, *Institute of Electrical and Electronics Engineers (IEEE) Press*, New Jersey, John Wiley and Son, Inc. 2013. ISBN 978-1-118-02429-4

[19] Ong, C. "Dynamic Simulation of Electric Machinery Using Matlab and Simulink", *Prentice Hall PTR*, New Jersey, 1997. ISBN: 978-0-13-723785-2

.